The International Association for the Properties of Water and Steam

Moscow, Russia
June 2014

Revised Supplementary Release on Backward Equations for the Functions *T*(*p*,*h*), *v*(*p*,*h*) and *T*(*p*,*s*), *v*(*p*,*s*) for Region 3 of the IAPWS Industrial Formulation 1997 for the Thermodynamic Properties of Water and Steam

President:
Professor Tamara Petrova
Moscow Engineering Power Institute
Moscow, Russia

Executive Secretary:
Dr. R. B. Dooley
Structural Integrity Associates
Southport, Merseyside, UK
Email: bdooley@structint.com

This revised supplementary release replaces the corresponding revised supplementary release of 2004, and contains 22 pages, including this cover page.

This revised supplementary release has been authorized by the International Association for the Properties of Water and Steam (IAPWS) at its meeting in Moscow, Russia, 22-27 June, 2014, for issue by its Secretariat. The members of IAPWS are: Britain and Ireland, Canada, the Czech Republic, Germany, Japan, Russia, Scandinavia (Denmark, Finland, Norway, Sweden), and the United States, and associate members Argentina & Brazil, Australia, France, Greece, Italy, New Zealand, and Switzerland.

The backward equations for temperature and specific volume as functions of pressure and enthalpy $T(p,h)$, $v(p,h)$ and as functions of pressure and entropy $T(p,s)$, $v(p,s)$ for region 3, and the equations for saturation pressure as a function of enthalpy $p_{3\mathrm{sat}}(h)$ and as a function of entropy $p_{3\mathrm{sat}}(s)$ for the saturation boundaries of region 3 provided in this release are recommended as a supplement to "IAPWS Industrial Formulation 1997 for the Thermodynamic Properties of Water and Steam" (IAPWS-IF97) [1, 2]. Further details concerning the equations can be found in the corresponding article by H.-J. Kretzschmar et al. [3].

This revision consists of edits to clarify descriptions of how to determine the region or subregion; the property calculations are unchanged.

Further information concerning this supplementary release, other releases, supplementary releases, guidelines, technical guidance documents, and advisory notes issued by IAPWS can be obtained from the Executive Secretary of IAPWS or from http://www.iapws.org.

Contents

1 Nomenclature

Thermodynamic quantities:

f	Specific Helmholtz free energy
h	Specific enthalpy
p	Pressure
s	Specific entropy
T	Absolute temperature [a]
v	Specific volume
Δ	Difference in any quantity
η	Reduced enthalpy, $\eta = h/h^*$
θ	Reduced temperature $\theta = T/T^*$
π	Reduced pressure, $\pi = p/p^*$
ρ	Density
σ	Reduced entropy, $\sigma = s/s^*$
ω	Reduced volume, $\omega = v/v^*$
x	Vapor fraction

Root-mean-square value:

$$\Delta x_{RMS} = \sqrt{\frac{1}{N}\sum_{n=1}^{N}(\Delta x_n)^2}$$

where Δx_n can be either absolute or percentage difference between the corresponding quantities x; N is the number of Δx_n values (100 million points uniformly distributed over the range of validity in the p-T plane).

Superscripts:

01	Equation of IAPWS-IF97-S01
97	Quantity or equation of IAPWS-IF97
*	Reducing quantity
'	Saturated liquid state
"	Saturated vapor state

Subscripts:

1	Region 1
2	Region 2
3	Region 3
3a	Subregion 3a
3b	Subregion 3b
3ab	Boundary between subregions 3a and 3b
4	Region 4
5	Region 5
B23	Boundary between regions 2 and 3
c	Critical point
it	Iterated quantity
max	Maximum value of a quantity
RMS	Root-mean-square value of a quantity
sat	Saturation state
tol	Tolerance, range of accepted value of a quantity

[a] Note: T denotes absolute temperature on the International Temperature Scale of 1990 (ITS-90).

2 Background

The Industrial Formulation IAPWS-IF97 for the thermodynamic properties of water and steam [1, 2] contains basic equations, saturation equations and equations for the most often used backward functions $T(p,h)$ and $T(p,s)$ valid in the liquid region 1 and the vapor region 2; see Figure 1. The IAPWS-IF97 was supplemented by "Backward Equations for Pressure as a Function of Enthalpy and Entropy $p(h,s)$ to the Industrial Formulation 1997 for the Thermodynamic Properties of Water and Steam" [4, 5], which is referred to here as IAPWS-IF97-S01, including equations for the backward function $p(h,s)$ valid in region 1 and region 2.

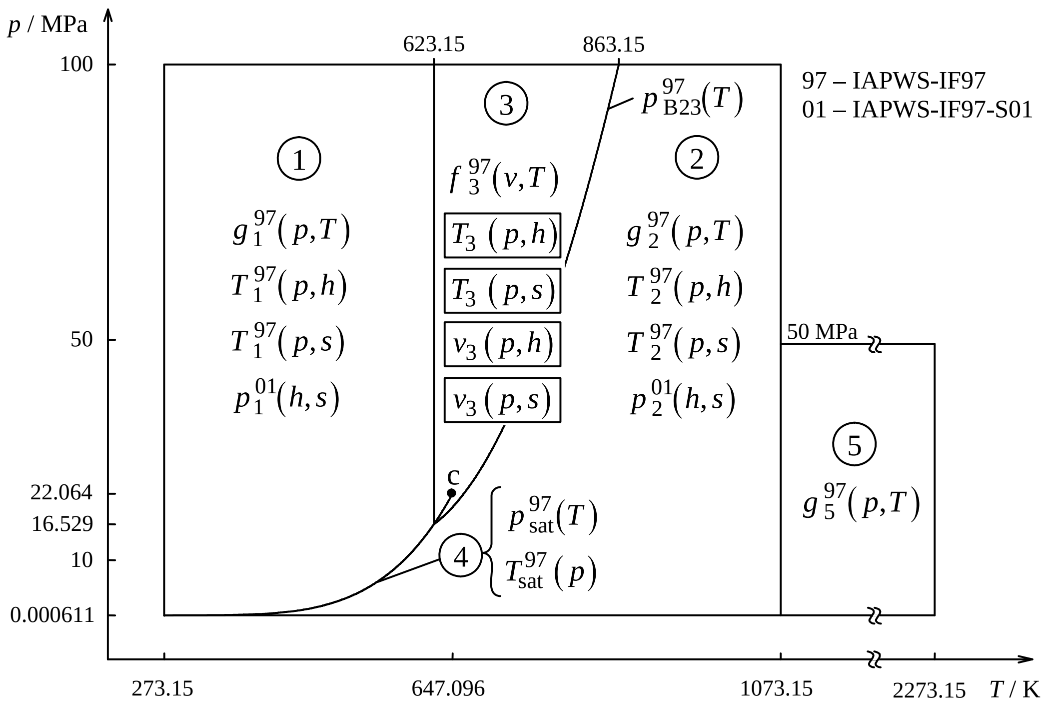

Figure 1. Regions and equations of IAPWS-IF97, IAPWS-IF97-S01, and the backward equations $T(p,h)$, $v(p,h)$, and $T(p,s)$, $v(p,s)$ of this release

In modeling steam power cycles, thermodynamic properties as functions of the variables (p,h) or (p,s) are also required in region 3. It is difficult to perform these calculations with IAPWS-IF97, because two-dimensional iteration is required using the functions $p(v,T)$, $h(v,T)$ or $p(v,T)$, $s(v,T)$ that can be explicitly calculated from the fundamental region 3 equation $f(v,T)$. While these calculations are not frequently required in region 3, the relatively large computing time required for two-dimensional iteration can be significant in process modeling.

In order to avoid such iterations, this release provides equations for the backward functions $T_3(p,h)$, $v_3(p,h)$ and $T_3(p,s)$, $v_3(p,s)$, see Figure 1. With temperature and specific volume calculated from the backward equations, the other properties in region 3 can be calculated using the IAPWS-IF97 basic equation $f_3^{97}(v,T)$.

In addition, boundary equations for the saturation pressure as a function of enthalpy $p_{3\mathrm{sat}}(h)$ and as a function of entropy $p_{3\mathrm{sat}}(s)$ for the saturated liquid and vapor lines of region 3 are provided. Using these equations, whether a state point is located in the single-phase region or in the two-phase (wet steam) region can be determined without iteration. Section 4 contains the comprehensive description of the boundary equations.

The numerical consistencies of all backward equations and boundary equations presented in Sections 3 and 4 with the IAPWS-IF97 basic equation are sufficient for most applications in heat cycle and steam turbine calculations. For applications where the demands on numerical consistency are extremely high, iterations using the IAPWS-IF97 basic equation may be necessary. In these cases, the backward or boundary equations can be used for calculating very accurate starting values. The time required to reach the convergence criteria of the iteration will be significantly reduced.

The presented backward and boundary equations can only be used in their ranges of validity described in Sections 3.2, 4.3, and 4.4. They should not be used for determining any thermodynamic derivatives.

In any case, depending on the application, a conscious decision is required whether to use the backward or boundary equations or to calculate the corresponding values by iterations from the basic equation of IAPWS-IF97.

3 Backward Equations *T*(*p*,*h*), *v*(*p*,*h*), *T*(*p*,*s*), and *v*(*p*,*s*) for Region 3

3.1 Numerical Consistency Requirements

The permissible value for the numerical consistency $|\Delta T|_{\mathrm{tol}} = 25\ \mathrm{mK}$ of the backward functions $T_3(p,h)$ and $T_3(p,s)$ with the basic equation $f_3^{97}(v,T)$ was determined by IAPWS [6, 7] as a result of an international survey.

The permissible value Δv_{tol} for the numerical consistency for the equations $v_3(p,h)$ and $v_3(p,s)$ can be estimated from the total differentials

$$\Delta v_{\mathrm{tol}} = \left(\frac{\partial v}{\partial T}\right)_h \Delta T_{\mathrm{tol}} + \left(\frac{\partial v}{\partial h}\right)_T \Delta h_{\mathrm{tol}} \quad \text{and} \quad \Delta v_{\mathrm{tol}} = \left(\frac{\partial v}{\partial T}\right)_s \Delta T_{\mathrm{tol}} + \left(\frac{\partial v}{\partial s}\right)_T \Delta s_{\mathrm{tol}} \ ,$$

where $\left(\frac{\partial v}{\partial T}\right)_h$, $\left(\frac{\partial v}{\partial h}\right)_T$, $\left(\frac{\partial v}{\partial T}\right)_s$, and $\left(\frac{\partial v}{\partial s}\right)_T$ are derivatives [8] calculated from the IAPWS-IF97 basic equation and Δh_{tol} and Δs_{tol} are values determined by IAPWS for the adjacent region 1 and subregion 2c [9], see Table 1. The resulting permissible specific volume difference is $\left|\Delta v/v\right|_{\text{tol}} = 0.01\,\%$ for both functions $v_3\left(p,h\right)$ and $v_3\left(p,s\right)$.

At the critical point $\left[T_\text{c} = 647.096\,\text{K},\, v_\text{c} = 1/\left(322\ \text{kg m}^{-3}\right)\right]$ [10], more stringent consistency requirements were arbitrarily set. These were $\left|\Delta T\right|_{\text{tol}} = 0.49\ \text{mK}$ and $\left|\Delta v/v\right|_{\text{tol}} = 0.0001\,\%$.

Table 1. Numerical consistency values $\left|\Delta T\right|_{\text{tol}}$ of [6] required for $T_3\left(p,h\right)$ and $T_3\left(p,s\right)$, values $\left|\Delta h\right|_{\text{tol}}$, $\left|\Delta s\right|_{\text{tol}}$ of [9], and resulting tolerances $\left|\Delta v/v\right|_{\text{tol}}$ required for $v_3\left(p,h\right)$ and $v_3\left(p,s\right)$

	$\left\|\Delta T\right\|_{\text{tol}}$	$\left\|\Delta h\right\|_{\text{tol}}$	$\left\|\Delta s\right\|_{\text{tol}}$	$\left\|\Delta v/v\right\|_{\text{tol}}$
Region 3	25 mK	80 J kg^{-1}	0.1 J kg^{-1} K^{-1}	0.01 %
Critical Point	0.49 mK	-	-	0.0001 %

3.2 Structure of the Equation Set

The equation set consists of backward equations $T\left(p,h\right)$, $v\left(p,h\right)$ and $T\left(p,s\right)$, $v\left(p,s\right)$ for region 3. Region 3 is defined by:

$$623.15\ \text{K} \le T \le 863.15\ \text{K} \quad \text{and} \quad p_{\text{B23}}^{97}(T) \le p \le 100\ \text{MPa}\,,$$

where p_{B23}^{97} represents the B23 equation of IAPWS-IF97. Figure 2 shows the way in which region 3 is divided into the two subregions 3a and 3b.

The boundary between the subregions 3a and 3b corresponds to the critical isentropic line

$$s = s_\text{c} = 4.412\ 021\ 482\ 234\ 76\ \text{kJ kg}^{-1}\ \text{K}^{-1};$$

see Figure 2. For the functions $T\left(p,s\right)$ and $v\left(p,s\right)$, input points can be tested directly to identify the subregion since the specific entropy is an independent variable.

In order to decide which $T\left(p,h\right)$, $v\left(p,h\right)$ equation, 3a or 3b, must be used for given values of p and h, the boundary equation $h_{\text{3ab}}\left(p\right)$, Eq. (1), has to be used; see Figure 2. This equation is a polynomial of the third degree and reads

$$\frac{h_{\text{3ab}}\left(p\right)}{h^*} = \eta(\pi) = n_1 + n_2\pi + n_3\pi^2 + n_4\pi^3\ , \tag{1}$$

where $\eta = h/h^*$ and $\pi = p/p^*$ with $h^* = 1\,\text{kJ kg}^{-1}$ and $p^* = 1\,\text{MPa}$. The coefficients n_1 to n_4 of Eq. (1) are listed in Table 2. The range of the equation $h_{\text{3ab}}\left(p\right)$ is from the critical point to 100 MPa. The related temperature at 100 MPa is $T = 762.380\ 873\ 481$ K. Equation (1) does not exactly describe the critical isentropic line.

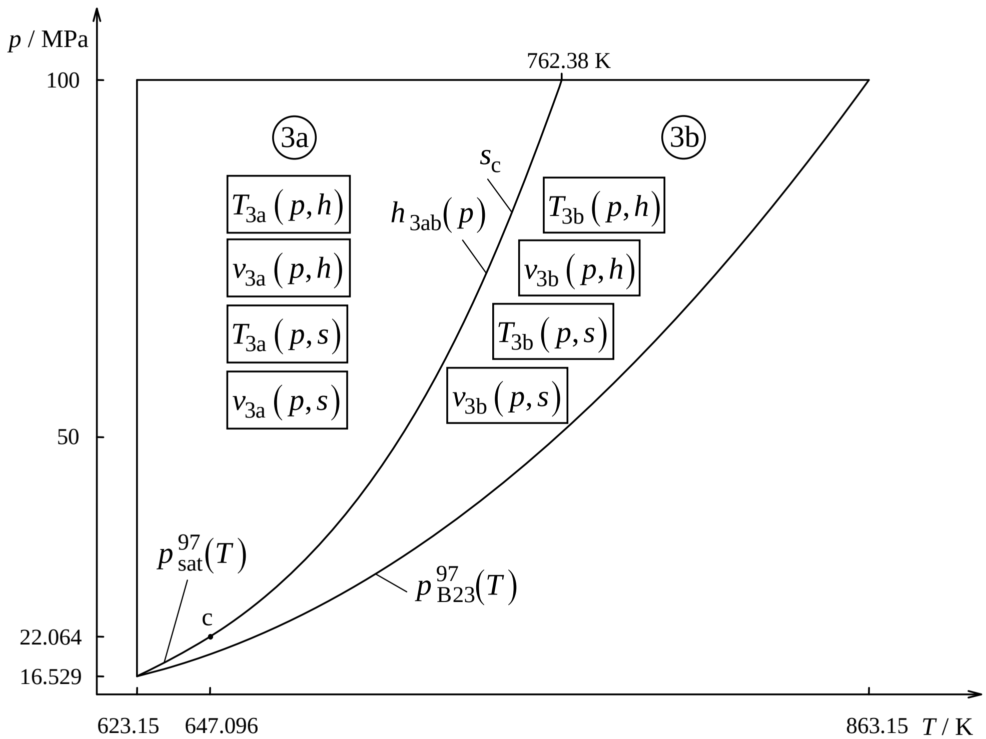

Figure 2. Division of region 3 into two subregions 3a and 3b for the backward equations $T(p,h)$, $v(p,h)$ and $T(p,s)$, $v(p,s)$

Table 2. Numerical values of the coefficients of the equation $h_{3ab}(p)$ in its dimensionless form, Eq. (1), for defining the boundary between subregions 3a and 3b

i	n_i	i	n_i
1	$0.201\,464\,004\,206\,875 \times 10^{4}$	3	$-0.219\,921\,901\,054\,187 \times 10^{-1}$
2	$0.374\,696\,550\,136\,983 \times 10^{1}$	4	$0.875\,131\,686\,009\,950 \times 10^{-4}$

The maximum specific entropy deviation was determined as

$$\left|\Delta s_{3ab}\right|_{max} = \left| s_3^{97}\left(T_{it}^{97}\left(p, h_{3ab}(p)\right), v_{it}^{97}\left(p, h_{3ab}(p)\right)\right) - s_c \right|_{max} = 0.66\ \mathrm{J\,kg^{-1}\,K^{-1}}\ ,$$

where T_{it}^{97} and v_{it}^{97} were obtained by iterations using the derivatives $p_3^{97}(v,T)$ and $s_3^{97}(v,T)$ of the IAPWS-IF97 basic equation for region 3.

Equation (1) does not correctly reproduce the isentropic line $s = s_c$ at pressures lower than p_c. However, the calculated values $h_{3ab}(p)$ are not higher than the enthalpy on the saturated vapor line and not lower than the enthalpy on the saturated liquid line.

For *computer-program verification*, Eq. (1) gives the following *p*-*h* point:

$$p = 25\ \text{MPa}\,,\ h_{3ab}(p) = 2.095\,936\,454 \times 10^3\ \text{kJ kg}^{-1}.$$

3.3 Backward Equations *T*(*p*,*h*) and *v*(*p*,*h*) for Subregions 3a and 3b

The Equations T(p,h). The backward equation $T_{3a}(p,h)$ for subregion 3a has the following dimensionless form:

$$\frac{T_{3a}(p,h)}{T^*} = \theta_{3a}(\pi,\eta) = \sum_{i=1}^{31} n_i\,(\pi + 0.240)^{I_i}\,(\eta - 0.615)^{J_i}\ , \tag{2}$$

where $\theta = T/T^*$, $\pi = p/p^*$, and $\eta = h/h^*$, with $T^* = 760\ \text{K}$, $p^* = 100\ \text{MPa}$, and $h^* = 2300\ \text{kJ kg}^{-1}$. The coefficients n_i and exponents I_i and J_i of Eq. (2) are listed in Table 3.

The backward equation $T_{3b}(p,h)$ for subregion 3b reads in its dimensionless form

$$\frac{T_{3b}(p,h)}{T^*} = \theta_{3b}(\pi,\eta) = \sum_{i=1}^{33} n_i\,(\pi + 0.298)^{I_i}\,(\eta - 0.720)^{J_i}\ , \tag{3}$$

where $\theta = T/T^*$, $\pi = p/p^*$, and $\eta = h/h^*$, with $T^* = 860\ \text{K}$, $p^* = 100\ \text{MPa}$, and $h^* = 2800\ \text{kJ kg}^{-1}$. The coefficients n_i and exponents I_i and J_i of Eq. (3) are listed in Table 4.

Table 3. Coefficients and exponents of the backward equation $T_{3a}(p,h)$ for subregion 3a in its dimensionless form, Eq. (2)

i	I_i	J_i	n_i	i	I_i	J_i	n_i
1	−12	0	$-0.133\,645\,667\,811\,215 \times 10^{-6}$	17	−3	0	$-0.384\,460\,997\,596\,657 \times 10^{-5}$
2	−12	1	$0.455\,912\,656\,802\,978 \times 10^{-5}$	18	−2	1	$0.337\,423\,807\,911\,655 \times 10^{-2}$
3	−12	2	$-0.146\,294\,640\,700\,979 \times 10^{-4}$	19	−2	3	$-0.551\,624\,873\,066\,791$
4	−12	6	$0.639\,341\,312\,970\,080 \times 10^{-2}$	20	−2	4	$0.729\,202\,277\,107\,470$
5	−12	14	$0.372\,783\,927\,268\,847 \times 10^{3}$	21	−1	0	$-0.992\,522\,757\,376\,041 \times 10^{-2}$
6	−12	16	$-0.718\,654\,377\,460\,447 \times 10^{4}$	22	−1	2	$-0.119\,308\,831\,407\,288$
7	−12	20	$0.573\,494\,752\,103\,400 \times 10^{6}$	23	0	0	$0.793\,929\,190\,615\,421$
8	−12	22	$-0.267\,569\,329\,111\,439 \times 10^{7}$	24	0	1	$0.454\,270\,731\,799\,386$
9	−10	1	$-0.334\,066\,283\,302\,614 \times 10^{-4}$	25	1	1	$0.209\,998\,591\,259\,910$
10	−10	5	$-0.245\,479\,214\,069\,597 \times 10^{-1}$	26	3	0	$-0.642\,109\,823\,904\,738 \times 10^{-2}$
11	−10	12	$0.478\,087\,847\,764\,996 \times 10^{2}$	27	3	1	$-0.235\,155\,868\,604\,540 \times 10^{-1}$
12	−8	0	$0.764\,664\,131\,818\,904 \times 10^{-5}$	28	4	0	$0.252\,233\,108\,341\,612 \times 10^{-2}$
13	−8	2	$0.128\,350\,627\,676\,972 \times 10^{-2}$	29	4	3	$-0.764\,885\,133\,368\,119 \times 10^{-2}$
14	−8	4	$0.171\,219\,081\,377\,331 \times 10^{-1}$	30	10	4	$0.136\,176\,427\,574\,291 \times 10^{-1}$
15	−8	10	$-0.851\,007\,304\,583\,213 \times 10^{1}$	31	12	5	$-0.133\,027\,883\,575\,669 \times 10^{-1}$
16	−5	2	$-0.136\,513\,461\,629\,781 \times 10^{-1}$				

Table 4. Coefficients and exponents of the backward equation $T_{3b}(p,h)$ for subregion 3b in its dimensionless form, Eq. (3)

i	I_i	J_i	n_i	i	I_i	J_i	n_i
1	−12	0	$0.323\,254\,573\,644\,920 \times 10^{-4}$	18	−3	5	$-0.307\,622\,221\,350\,501 \times 10^{1}$
2	−12	1	$-0.127\,575\,556\,587\,181 \times 10^{-3}$	19	−2	0	$-0.574\,011\,959\,864\,879 \times 10^{-1}$
3	−10	0	$-0.475\,851\,877\,356\,068 \times 10^{-3}$	20	−2	4	$0.503\,471\,360\,939\,849 \times 10^{1}$
4	−10	1	$0.156\,183\,014\,181\,602 \times 10^{-2}$	21	−1	2	$-0.925\,081\,888\,584\,834$
5	−10	5	$0.105\,724\,860\,113\,781$	22	−1	4	$0.391\,733\,882\,917\,546 \times 10^{1}$
6	−10	10	$-0.858\,514\,221\,132\,534 \times 10^{2}$	23	−1	6	$-0.773\,146\,007\,130\,190 \times 10^{2}$
7	−10	12	$0.724\,140\,095\,480\,911 \times 10^{3}$	24	−1	10	$0.949\,308\,762\,098\,587 \times 10^{4}$
8	−8	0	$0.296\,475\,810\,273\,257 \times 10^{-2}$	25	−1	14	$-0.141\,043\,719\,679\,409 \times 10^{7}$
9	−8	1	$-0.592\,721\,983\,365\,988 \times 10^{-2}$	26	−1	16	$0.849\,166\,230\,819\,026 \times 10^{7}$
10	−8	2	$-0.126\,305\,422\,818\,666 \times 10^{-1}$	27	0	0	$0.861\,095\,729\,446\,704$
11	−8	4	$-0.115\,716\,196\,364\,853$	28	0	2	$0.323\,346\,442\,811\,720$
12	−8	10	$0.849\,000\,969\,739\,595 \times 10^{2}$	29	1	1	$0.873\,281\,936\,020\,439$
13	−6	0	$-0.108\,602\,260\,086\,615 \times 10^{-1}$	30	3	1	$-0.436\,653\,048\,526\,683$
14	−6	1	$0.154\,304\,475\,328\,851 \times 10^{-1}$	31	5	1	$0.286\,596\,714\,529\,479$
15	−6	2	$0.750\,455\,441\,524\,466 \times 10^{-1}$	32	6	1	$-0.131\,778\,331\,276\,228$
16	−4	0	$0.252\,520\,973\,612\,982 \times 10^{-1}$	33	8	1	$0.676\,682\,064\,330\,275 \times 10^{-2}$
17	−4	1	$-0.602\,507\,901\,232\,996 \times 10^{-1}$				

Computer-program verification. To assist the user in computer-program verification of Eqs. (2) and (3), Table 5 contains test values for calculated temperatures.

Table 5. Selected temperature values calculated from Eqs. (2) and (3) [a]

Equation	p / MPa	h / kJ kg^{-1}	T / K
	20	1700	$6.293\,083\,892 \times 10^{2}$
$T_{3a}(p,h)$, Eq. (2)	50	2000	$6.905\,718\,338 \times 10^{2}$
	100	2100	$7.336\,163\,014 \times 10^{2}$
	20	2500	$6.418\,418\,053 \times 10^{2}$
$T_{3b}(p,h)$, Eq. (3)	50	2400	$7.351\,848\,618 \times 10^{2}$
	100	2700	$8.420\,460\,876 \times 10^{2}$

[a] It is recommended that programmed functions be verified using 8 byte real values for all variables.

The Equations v(p,h). The backward equation $v_{3a}(p,h)$ for subregion 3a has the following dimensionless form:

$$\frac{v_{3a}(p,h)}{v^*} = \omega_{3a}(\pi,\eta) = \sum_{i=1}^{32} n_i\,(\pi + 0.128)^{I_i}\,(\eta - 0.727)^{J_i}\ , \tag{4}$$

where $\omega = v/v^*$, $\pi = p/p^*$, and $\eta = h/h^*$, with $v^* = 0.0028\ \mathrm{m^3\ kg^{-1}}$, $p^* = 100\ \mathrm{MPa}$, and $h^* = 2100\ \mathrm{kJ\ kg^{-1}}$. The coefficients n_i and exponents I_i and J_i of Eq. (4) are listed in Table 6.

The backward equation $v_{3b}(p,h)$ for subregion 3b reads in its dimensionless form

$$\frac{v_{3b}(p,h)}{v^*} = \omega_{3b}(\pi,\eta) = \sum_{i=1}^{30} n_i \left(\pi + 0.0661\right)^{I_i} \left(\eta - 0.720\right)^{J_i} , \tag{5}$$

where $\omega = v/v^*$, $\pi = p/p^*$, and $\eta = h/h^*$, with $v^* = 0.0088\ \mathrm{m^3\ kg^{-1}}$, $p^* = 100\ \mathrm{MPa}$, and $h^* = 2800\ \mathrm{kJ\ kg^{-1}}$. The coefficients n_i and exponents I_i and J_i of Eq. (5) are listed in Table 7.

Table 6. Coefficients and exponents of the backward equation $v_{3a}(p,h)$ for subregion 3a in its dimensionless form, Eq. (4)

i	I_i	J_i	n_i	i	I_i	J_i	n_i
1	−12	6	$0.529\,944\,062\,966\,028 \times 10^{-2}$	17	−2	16	$0.568\,366\,875\,815\,960 \times 10^{4}$
2	−12	8	$-0.170\,099\,690\,234\,461$	18	−1	0	$0.808\,169\,540\,124\,668 \times 10^{-2}$
3	−12	12	$0.111\,323\,814\,312\,927 \times 10^{2}$	19	−1	1	$0.172\,416\,341\,519\,307$
4	−12	18	$-0.217\,898\,123\,145\,125 \times 10^{4}$	20	−1	2	$0.104\,270\,175\,292\,927 \times 10^{1}$
5	−10	4	$-0.506\,061\,827\,980\,875 \times 10^{-3}$	21	−1	3	$-0.297\,691\,372\,792\,847$
6	−10	7	$0.556\,495\,239\,685\,324$	22	0	0	$0.560\,394\,465\,163\,593$
7	−10	10	$-0.943\,672\,726\,094\,016 \times 10^{1}$	23	0	1	$0.275\,234\,661\,176\,914$
8	−8	5	$-0.297\,856\,807\,561\,527$	24	1	0	$-0.148\,347\,894\,866\,012$
9	−8	12	$0.939\,353\,943\,717\,186 \times 10^{2}$	25	1	1	$-0.651\,142\,513\,478\,515 \times 10^{-1}$
10	−6	3	$0.192\,944\,939\,465\,981 \times 10^{-1}$	26	1	2	$-0.292\,468\,715\,386\,302 \times 10^{1}$
11	−6	4	$0.421\,740\,664\,704\,763$	27	2	0	$0.664\,876\,096\,952\,665 \times 10^{-1}$
12	−6	22	$-0.368\,914\,126\,282\,330 \times 10^{7}$	28	2	2	$0.352\,335\,014\,263\,844 \times 10^{1}$
13	−4	2	$-0.737\,566\,847\,600\,639 \times 10^{-2}$	29	3	0	$-0.146\,340\,792\,313\,332 \times 10^{-1}$
14	−4	3	$-0.354\,753\,242\,424\,366$	30	4	2	$-0.224\,503\,486\,668\,184 \times 10^{1}$
15	−3	7	$-0.199\,768\,169\,338\,727 \times 10^{1}$	31	5	2	$0.110\,533\,464\,706\,142 \times 10^{1}$
16	−2	3	$0.115\,456\,297\,059\,049 \times 10^{1}$	32	8	2	$-0.408\,757\,344\,495\,612 \times 10^{-1}$

Table 7. Coefficients and exponents of the backward equation $v_{3b}(p,h)$ for subregion 3b in its dimensionless form, Eq. (5)

i	I_i	J_i	n_i	i	I_i	J_i	n_i
1	−12	0	$-0.225\,196\,934\,336\,318 \times 10^{-8}$	16	−4	6	$-0.321\,087\,965\,668\,917 \times 10^{1}$
2	−12	1	$0.140\,674\,363\,313\,486 \times 10^{-7}$	17	−4	10	$0.607\,567\,815\,637\,771 \times 10^{3}$
3	−8	0	$0.233\,784\,085\,280\,560 \times 10^{-5}$	18	−3	0	$0.557\,686\,450\,685\,932 \times 10^{-3}$
4	−8	1	$-0.331\,833\,715\,229\,001 \times 10^{-4}$	19	−3	2	$0.187\,499\,040\,029\,550$
5	−8	3	$0.107\,956\,778\,514\,318 \times 10^{-2}$	20	−2	1	$0.905\,368\,030\,448\,107 \times 10^{-2}$
6	−8	6	$-0.271\,382\,067\,378\,863$	21	−2	2	$0.285\,417\,173\,048\,685$
7	−8	7	$0.107\,202\,262\,490\,333 \times 10^{1}$	22	−1	0	$0.329\,924\,030\,996\,098 \times 10^{-1}$
8	−8	8	$-0.853\,821\,329\,075\,382$	23	−1	1	$0.239\,897\,419\,685\,483$
9	−6	0	$-0.215\,214\,194\,340\,526 \times 10^{-4}$	24	−1	4	$0.482\,754\,995\,951\,394 \times 10^{1}$
10	−6	1	$0.769\,656\,088\,222\,730 \times 10^{-3}$	25	−1	5	$-0.118\,035\,753\,702\,231 \times 10^{2}$
11	−6	2	$-0.431\,136\,580\,433\,864 \times 10^{-2}$	26	0	0	$0.169\,490\,044\,091\,791$
12	−6	5	$0.453\,342\,167\,309\,331$	27	1	0	$-0.179\,967\,222\,507\,787 \times 10^{-1}$
13	−6	6	$-0.507\,749\,535\,873\,652$	28	1	1	$0.371\,810\,116\,332\,674 \times 10^{-1}$
14	−6	10	$-0.100\,475\,154\,528\,389 \times 10^{3}$	29	2	2	$-0.536\,288\,335\,065\,096 \times 10^{-1}$
15	−4	3	$-0.219\,201\,924\,648\,793$	30	2	6	$0.160\,697\,101\,092\,520 \times 10^{1}$

Computer-program verification. To assist the user in computer-program verification of Eqs. (4) and (5), Table 8 contains test values for calculated specific volumes.

Table 8. Selected specific volume values calculated from Eqs. (4) and (5) [a]

Equation	p / MPa	h / kJ kg^{-1}	v / m^3 kg^{-1}
$v_{3a}(p,h)$, Eq. (4)	20	1700	$1.749\,903\,962 \times 10^{-3}$
	50	2000	$1.908\,139\,035 \times 10^{-3}$
	100	2100	$1.676\,229\,776 \times 10^{-3}$
$v_{3b}(p,h)$, Eq. (5)	20	2500	$6.670\,547\,043 \times 10^{-3}$
	50	2400	$2.801\,244\,590 \times 10^{-3}$
	100	2700	$2.404\,234\,998 \times 10^{-3}$

[a] It is recommended that programmed functions be verified using 8 byte real values for all variables.

Numerical Consistency with the Basic Equation of IAPWS-IF97. The maximum temperature differences and related root-mean-square differences between the calculated temperature Eqs. (2) and (3) and the IAPWS-IF97 basic equation $f_3^{97}(v,T)$ in comparison with the permissible differences are listed in Table 9. The calculation of the root-mean-square values is described in Section 1.

Table 9 also contains the maximum relative deviations and root-mean-square relative deviations for specific volume of Eqs. (4) and (5) from IAPWS-IF97.

The critical temperature and the critical volume are met exactly by the equations $T(p,h)$ and $v(p,h)$.

Table 9. Maximum differences and root-mean-square differences of the temperature calculated from Eqs. (2) and (3) and specific volume calculated from Eqs. (4) and (5) to the IAPWS-IF97 basic equation $f_3^{97}(v,T)$ and related permissible values

Subregion	Equation	$\lvert\Delta T\rvert_{\text{tol}}$	$\lvert\Delta T\rvert_{\max}$	$\lvert\Delta T\rvert_{\text{RMS}}$
3a	(2)	25 mK	23.6 mK	10.5 mK
3b	(3)	25 mK	19.6 mK	9.6 mK
Subregion	**Equation**	$\lvert\Delta v/v\rvert_{\text{tol}}$	$\lvert\Delta v/v\rvert_{\max}$	$\lvert\Delta v/v\rvert_{\text{RMS}}$
3a	(4)	0.01 %	0.0080 %	0.0032 %
3b	(5)	0.01 %	0.0095 %	0.0042 %

Consistency at Boundary Between Subregions. The maximum temperature difference between the two backward equations, Eq. (2) and Eq. (3), along the boundary $h_{3ab}(p)$, Eq. (1), has the following value

$$\lvert\Delta T\rvert_{\max} = \left| T_{3a}\left(p, h_{3ab}(p)\right) - T_{3b}\left(p, h_{3ab}(p)\right)\right|_{\max} = 0.37\,\text{mK}\,.$$

Thus, the temperature differences between the two backward functions $T(p,h)$ of the adjacent subregions are smaller than the numerical consistencies with the IAPWS-IF97 equations.

The relative specific volume differences between the two backward equations $v(p,h)$ of the adjacent subregions 3a and 3b are also smaller than the numerical consistencies of these equations with the IAPWS-IF97 basic equation. Along the boundary $h_{3\mathrm{ab}}(p)$, Eq. (1), the maximum difference between the corresponding equations was determined as:

$$\left|\frac{\Delta v}{v}\right|_{\max} = \left|\frac{v_{3\mathrm{a}}\left(p, h_{3\mathrm{ab}}(p)\right) - v_{3\mathrm{b}}\left(p, h_{3\mathrm{ab}}(p)\right)}{v_{3\mathrm{b}}\left(p, h_{3\mathrm{ab}}(p)\right)}\right|_{\max} = 0.00015\% \; .$$

3.4 Backward Equations *T*(*p*,*s*) and *v*(*p*,*s*) for Subregions 3a and 3b

The Equations T(p,s). The backward equation $T_{3\mathrm{a}}(p,s)$ for subregion 3a has the following dimensionless form:

$$\frac{T_{3\mathrm{a}}(p,s)}{T^*} = \theta_{3\mathrm{a}}(\pi,\sigma) = \sum_{i=1}^{33} n_i \left(\pi + 0.240\right)^{I_i} \left(\sigma - 0.703\right)^{J_i} \; , \tag{6}$$

where $\theta = T/T^*$, $\pi = p/p^*$, and $\sigma = s/s^*$, with $T^* = 760\ \mathrm{K}$, $p^* = 100\ \mathrm{MPa}$, and $s^* = 4.4\ \mathrm{kJ\ kg^{-1}\ K^{-1}}$. The coefficients n_i and exponents I_i and J_i of Eq. (6) are listed in Table 10.

The backward equation $T_{3\mathrm{b}}(p,s)$ for subregion 3b reads in its dimensionless form

$$\frac{T_{3\mathrm{b}}(p,s)}{T^*} = \theta_{3\mathrm{b}}(\pi,\sigma) = \sum_{i=1}^{28} n_i \left(\pi + 0.760\right)^{I_i} \left(\sigma - 0.818\right)^{J_i} \; , \tag{7}$$

where $\theta = T/T^*$, $\pi = p/p^*$, and $\sigma = s/s^*$, with $T^* = 860\ \mathrm{K}$, $p^* = 100\ \mathrm{MPa}$, and $s^* = 5.3\ \mathrm{kJ\ kg^{-1}\ K^{-1}}$. The coefficients n_i and exponents I_i and J_i of Eq. (7) are listed in Table 11.

Computer-program verification

To assist the user in computer-program verification of Eqs. (6) and (7), Table 12 contains test values for calculated temperatures.

Table 10. Coefficients and exponents of the backward equation $T_{3a}\left(p,s\right)$ for subregion 3a in its dimensionless form, Eq. (6)

i	I_i	J_i	n_i	i	I_i	J_i	n_i
1	−12	28	$0.150\,042\,008\,263\,875 \times 10^{10}$	18	−4	10	$-0.368\,275\,545\,889\,071 \times 10^{3}$
2	−12	32	$-0.159\,397\,258\,480\,424 \times 10^{12}$	19	−4	36	$0.664\,768\,904\,779\,177 \times 10^{16}$
3	−10	4	$0.502\,181\,140\,217\,975 \times 10^{-3}$	20	−2	1	$0.449\,359\,251\,958\,880 \times 10^{-1}$
4	−10	10	$-0.672\,057\,767\,855\,466 \times 10^{2}$	21	−2	4	$-0.422\,897\,836\,099\,655 \times 10^{1}$
5	−10	12	$0.145\,058\,545\,404\,456 \times 10^{4}$	22	−1	1	$-0.240\,614\,376\,434\,179$
6	−10	14	$-0.823\,889\,534\,888\,890 \times 10^{4}$	23	−1	6	$-0.474\,341\,365\,254\,924 \times 10^{1}$
7	−8	5	$-0.154\,852\,214\,233\,853$	24	0	0	$0.724\,093\,999\,126\,110$
8	−8	7	$0.112\,305\,046\,746\,695 \times 10^{2}$	25	0	1	$0.923\,874\,349\,695\,897$
9	−8	8	$-0.297\,000\,213\,482\,822 \times 10^{2}$	26	0	4	$0.399\,043\,655\,281\,015 \times 10^{1}$
10	−8	28	$0.438\,565\,132\,635\,495 \times 10^{11}$	27	1	0	$0.384\,066\,651\,868\,009 \times 10^{-1}$
11	−6	2	$0.137\,837\,838\,635\,464 \times 10^{-2}$	28	2	0	$-0.359\,344\,365\,571\,848 \times 10^{-2}$
12	−6	6	$-0.297\,478\,527\,157\,462 \times 10^{1}$	29	2	3	$-0.735\,196\,448\,821\,653$
13	−6	32	$0.971\,777\,947\,349\,413 \times 10^{13}$	30	3	2	$0.188\,367\,048\,396\,131$
14	−5	0	$-0.571\,527\,767\,052\,398 \times 10^{-4}$	31	8	0	$0.141\,064\,266\,818\,704 \times 10^{-3}$
15	−5	14	$0.288\,307\,949\,778\,420 \times 10^{5}$	32	8	1	$-0.257\,418\,501\,496\,337 \times 10^{-2}$
16	−5	32	$-0.744\,428\,289\,262\,703 \times 10^{14}$	33	10	2	$0.123\,220\,024\,851\,555 \times 10^{-2}$
17	−4	6	$0.128\,017\,324\,848\,921 \times 10^{2}$				

Table 11. Coefficients and exponents of the backward equation $T_{3b}\left(p,s\right)$ for subregion 3b in its dimensionless form, Eq. (7)

i	I_i	J_i	n_i	i	I_i	J_i	n_i
1	−12	1	$0.527\,111\,701\,601\,660$	15	−5	6	$0.880\,531\,517\,490\,555 \times 10^{3}$
2	−12	3	$-0.401\,317\,830\,052\,742 \times 10^{2}$	16	−4	12	$0.265\,015\,592\,794\,626 \times 10^{7}$
3	−12	4	$0.153\,020\,073\,134\,484 \times 10^{3}$	17	−3	1	$-0.359\,287\,150\,025\,783$
4	−12	7	$-0.224\,799\,398\,218\,827 \times 10^{4}$	18	−3	6	$-0.656\,991\,567\,673\,753 \times 10^{3}$
5	−8	0	$-0.193\,993\,484\,669\,048$	19	−2	2	$0.241\,768\,149\,185\,367 \times 10^{1}$
6	−8	1	$-0.140\,467\,557\,893\,768 \times 10^{1}$	20	0	0	$0.856\,873\,461\,222\,588$
7	−8	3	$0.426\,799\,878\,114\,024 \times 10^{2}$	21	2	1	$0.655\,143\,675\,313\,458$
8	−6	0	$0.752\,810\,643\,416\,743$	22	3	1	$-0.213\,535\,213\,206\,406$
9	−6	2	$0.226\,657\,238\,616\,417 \times 10^{2}$	23	4	0	$0.562\,974\,957\,606\,348 \times 10^{-2}$
10	−6	4	$-0.622\,873\,556\,909\,932 \times 10^{3}$	24	5	24	$-0.316\,955\,725\,450\,471 \times 10^{15}$
11	−5	0	$-0.660\,823\,667\,935\,396$	25	6	0	$-0.699\,997\,000\,152\,457 \times 10^{-3}$
12	−5	1	$0.841\,267\,087\,271\,658$	26	8	3	$0.119\,845\,803\,210\,767 \times 10^{-1}$
13	−5	2	$-0.253\,717\,501\,764\,397 \times 10^{2}$	27	12	1	$0.193\,848\,122\,022\,095 \times 10^{-4}$
14	−5	4	$0.485\,708\,963\,532\,948 \times 10^{3}$	28	14	2	$-0.215\,095\,749\,182\,309 \times 10^{-4}$

Table 12. Selected temperature values calculated from Eqs. (6) and (7)[a]

Equation	p / MPa	s / kJ kg^{-1} K^{-1}	T / K
	20	3.8	$6.282\,959\,869 \times 10^{2}$
$T_{3a}(p,s)$, Eq. (6)	50	3.6	$6.297\,158\,726 \times 10^{2}$
	100	4.0	$7.056\,880\,237 \times 10^{2}$
	20	5.0	$6.401\,176\,443 \times 10^{2}$
$T_{3b}(p,s)$, Eq. (7)	50	4.5	$7.163\,687\,517 \times 10^{2}$
	100	5.0	$8.474\,332\,825 \times 10^{2}$

[a] It is recommended that programmed functions be verified using 8 byte real values for all variables.

The Equations v(p,s). The backward equation $v_{3a}(p,s)$ for subregion 3a has the following dimensionless form:

$$\frac{v_{3a}(p,s)}{v^*} = \omega_{3a}(\pi,\sigma) = \sum_{i=1}^{28} n_i \,(\pi + 0.187)^{I_i}\,(\sigma - 0.755)^{J_i} \quad , \tag{8}$$

where $\omega = v/v^*$, $\pi = p/p^*$, and $\sigma = s/s^*$, with $v^* = 0.0028\ \mathrm{m^3\ kg^{-1}}$, $p^* = 100\ \mathrm{MPa}$, and $s^* = 4.4\ \mathrm{kJ\ kg^{-1}\ K^{-1}}$. The coefficients n_i and exponents I_i and J_i of Eq. (8) are listed in Table 13.

The backward equation $v_{3b}(p,s)$ for subregion 3b reads in its dimensionless form

$$\frac{v_{3b}(p,s)}{v^*} = \omega_{3b}(\pi,\sigma) = \sum_{i=1}^{31} n_i \,(\pi + 0.298)^{I_i}\,(\sigma - 0.816)^{J_i} \quad , \tag{9}$$

where $\omega = v/v^*$, $\pi = p/p^*$, and $\sigma = s/s^*$, with $v^* = 0.0088\ \mathrm{m^3\ kg^{-1}}$, $p^* = 100\ \mathrm{MPa}$, and $s^* = 5.3\ \mathrm{kJ\ kg^{-1}\ K^{-1}}$. The coefficients n_i and exponents I_i and J_i of Eq. (9) are listed in Table 14.

Computer-program verification. To assist the user in computer-program verification of Eqs. (8) and (9), Table 15 contains test values for calculated specific volumes.

Table 13. Coefficients and exponents of the backward equation $v_{3a}(p,s)$ for subregion 3a in its dimensionless form, Eq. (8).

i	I_i	J_i	n_i	i	I_i	J_i	n_i
1	−12	10	$0.795\,544\,074\,093\,975 \times 10^{2}$	15	−3	2	$-0.118\,008\,384\,666\,987$
2	−12	12	$-0.238\,261\,242\,984\,590 \times 10^{4}$	16	−3	4	$0.253\,798\,642\,355\,900 \times 10^{1}$
3	−12	14	$0.176\,813\,100\,617\,787 \times 10^{5}$	17	−2	3	$0.965\,127\,704\,669\,424$
4	−10	4	$-0.110\,524\,727\,080\,379 \times 10^{-2}$	18	−2	8	$-0.282\,172\,420\,532\,826 \times 10^{2}$
5	−10	8	$-0.153\,213\,833\,655\,326 \times 10^{2}$	19	−1	1	$0.203\,224\,612\,353\,823$
6	−10	10	$0.297\,544\,599\,376\,982 \times 10^{3}$	20	−1	2	$0.110\,648\,186\,063\,513 \times 10^{1}$
7	−10	20	$-0.350\,315\,206\,871\,242 \times 10^{8}$	21	0	0	$0.526\,127\,948\,451\,280$
8	−8	5	$0.277\,513\,761\,062\,119$	22	0	1	$0.277\,000\,018\,736\,321$
9	−8	6	$-0.523\,964\,271\,036\,888$	23	0	3	$0.108\,153\,340\,501\,132 \times 10^{1}$
10	−8	14	$-0.148\,011\,182\,995\,403 \times 10^{6}$	24	1	0	$-0.744\,127\,885\,357\,893 \times 10^{-1}$
11	−8	16	$0.160\,014\,899\,374\,266 \times 10^{7}$	25	2	0	$0.164\,094\,443\,541\,384 \times 10^{-1}$
12	−6	28	$0.170\,802\,322\,663\,427 \times 10^{13}$	26	4	2	$-0.680\,468\,275\,301\,065 \times 10^{-1}$
13	−5	1	$0.246\,866\,996\,006\,494 \times 10^{-3}$	27	5	2	$0.257\,988\,576\,101\,640 \times 10^{-1}$
14	−4	5	$0.165\,326\,084\,797\,980 \times 10^{1}$	28	6	0	$-0.145\,749\,861\,944\,416 \times 10^{-3}$

Table 14. Coefficients and exponents of the backward equation $v_{3b}(p,s)$ for subregion 3b in its dimensionless form, Eq. (9)

i	I_i	J_i	n_i	i	I_i	J_i	n_i
1	−12	0	$0.591\,599\,780\,322\,238 \times 10^{-4}$	17	−4	2	$-0.121\,613\,320\,606\,788 \times 10^{2}$
2	−12	1	$-0.185\,465\,997\,137\,856 \times 10^{-2}$	18	−4	3	$0.167\,637\,540\,957\,944 \times 10^{1}$
3	−12	2	$0.104\,190\,510\,480\,013 \times 10^{-1}$	19	−3	1	$-0.744\,135\,838\,773\,463 \times 10^{1}$
4	−12	3	$0.598\,647\,302\,038\,590 \times 10^{-2}$	20	−2	0	$0.378\,168\,091\,437\,659 \times 10^{-1}$
5	−12	5	$-0.771\,391\,189\,901\,699$	21	−2	1	$0.401\,432\,203\,027\,688 \times 10^{1}$
6	−12	6	$0.172\,549\,765\,557\,036 \times 10^{1}$	22	−2	2	$0.160\,279\,837\,479\,185 \times 10^{2}$
7	−10	0	$-0.467\,076\,079\,846\,526 \times 10^{-3}$	23	−2	3	$0.317\,848\,779\,347\,728 \times 10^{1}$
8	−10	1	$0.134\,533\,823\,384\,439 \times 10^{-1}$	24	−2	4	$-0.358\,362\,310\,304\,853 \times 10^{1}$
9	−10	2	$-0.808\,094\,336\,805\,495 \times 10^{-1}$	25	−2	12	$-0.115\,995\,260\,446\,827 \times 10^{7}$
10	−10	4	$0.508\,139\,374\,365\,767$	26	0	0	$0.199\,256\,573\,577\,909$
11	−8	0	$0.128\,584\,643\,361\,683 \times 10^{-2}$	27	0	1	$-0.122\,270\,624\,794\,624$
12	−5	1	$-0.163\,899\,353\,915\,435 \times 10^{1}$	28	0	2	$-0.191\,449\,143\,716\,586 \times 10^{2}$
13	−5	2	$0.586\,938\,199\,318\,063 \times 10^{1}$	29	1	0	$-0.150\,448\,002\,905\,284 \times 10^{-1}$
14	−5	3	$-0.292\,466\,667\,918\,613 \times 10^{1}$	30	1	2	$0.146\,407\,900\,162\,154 \times 10^{2}$
15	−4	0	$-0.614\,076\,301\,499\,537 \times 10^{-2}$	31	2	2	$-0.327\,477\,787\,188\,230 \times 10^{1}$
16	−4	1	$0.576\,199\,014\,049\,172 \times 10^{1}$				

Table 15. Selected specific volume values calculated from Eqs. (8) and (9) [a]

Equation	p / MPa	s / kJ kg^{-1} K^{-1}	v / m^3 kg^{-1}
$v_{3a}(p,s)$, Eq. (8)	20	3.8	$1.733\,791\,463 \times 10^{-3}$
	50	3.6	$1.469\,680\,170 \times 10^{-3}$
	100	4.0	$1.555\,893\,131 \times 10^{-3}$
$v_{3b}(p,s)$, Eq. (9)	20	5.0	$6.262\,101\,987 \times 10^{-3}$
	50	4.5	$2.332\,634\,294 \times 10^{-3}$
	100	5.0	$2.449\,610\,757 \times 10^{-3}$

[a] It is recommended that programmed functions be verified using 8 byte real values for all variables.

Numerical Consistency with the Basic Equation of IAPWS-IF97. The maximum temperature differences and related root-mean-square differences between the temperatures calculated from Eqs. (6) and (7) and the IAPWS-IF97 basic equation $f_3^{97}(v,T)$ in comparison with the permissible differences are listed in Table 16.

Table 16 also contains the maximum relative deviations and root-mean-square relative deviations for the specific volume of Eqs. (8) and (9) from IAPWS-IF97.

The critical temperature and the critical volume are met exactly by the equations $T(p,s)$ and $v(p,s)$.

Table 16. Maximum differences and root-mean-square differences of the temperature calculated from Eqs. (6) and (7), and specific volume calculated from Eqs. (8) and (9) from the IAPWS-IF97 basic equation $f_3^{97}(v,T)$, and related permissible values

Subregion	Equation	$\lvert\Delta T\rvert_{\mathrm{tol}}$	$\lvert\Delta T\rvert_{\max}$	$\lvert\Delta T\rvert_{\mathrm{RMS}}$
3a	(6)	25 mK	24.8 mK	11.2 mK
3b	(7)	25 mK	22.1 mK	10.1 mK
Subregion	Equation	$\lvert\Delta v/v\rvert_{\mathrm{tol}}$	$\lvert\Delta v/v\rvert_{\max}$	$\lvert\Delta v/v\rvert_{\mathrm{RMS}}$
3a	(8)	0.01 %	0.0096 %	0.0052 %
3b	(9)	0.01 %	0.0077 %	0.0037 %

Consistency at Boundary Between Subregions. The maximum temperature difference between the two backward equations, Eq. (6) and Eq. (7), along the boundary s_c, has the following value

$$|\Delta T|_{\max} = \left|T_{3a}(p,s_c) - T_{3b}(p,s_c)\right|_{\max} = 0.093\,\mathrm{mK}\,.$$

Thus, the temperature differences between the two backward functions $T(p,s)$ of the adjacent subregions are smaller than their differences with the IAPWS-IF97 equations.

The relative specific volume differences between the two backward equations $v(p,s)$, Eqs. (8) and (9), of the adjacent subregions are also smaller than the differences of these equations with the IAPWS-IF97 basic equation. Along the boundary s_c, the maximum difference between the corresponding equations was determined as

$$\left|\frac{\Delta v}{v}\right|_{\max} = \left|\frac{v_{3\mathrm{a}}\left(p,s_\mathrm{c}\right) - v_{3\mathrm{b}}\left(p,s_\mathrm{c}\right)}{v_{3\mathrm{b}}\left(p,s_\mathrm{c}\right)}\right|_{\max} = 0.00046\,\% \ .$$

3.5 Computing Time in Relation to IAPWS-IF97

A very important motivation for the development of the backward equations $T(p,h)$, $v(p,h)$ and $T(p,s)$, $v(p,s)$ for region 3 was reducing the computing time to obtain thermodynamic properties and differential quotients from given variables (p,h) and (p,s). In IAPWS-IF97, time-consuming iterations, *e.g.*, the two-dimensional Newton method, are required. Using the $T_3(p,h)$, $v_3(p,h)$, $T_3(p,s)$ and $v_3(p,s)$ equations, the calculation speed is about 20 times faster than that of the two-dimensional Newton method with convergence tolerances set to the values shown in Table 1.

The numerical consistency of T and v obtained in this way is sufficient for most heat cycle calculations.

For users not satisfied with the numerical consistency of the backward equations, the equations are still recommended for generating starting points for the iterative process. They will significantly reduce the time required to reach the convergence criteria of the iteration.

4 Boundary Equations $p_{\mathrm{sat}}(h)$ and $p_{\mathrm{sat}}(s)$ for the Saturation Lines of Region 3

4.1 Determination of the Region Boundaries for Given Variables (p,h) and (p,s)

The boundaries between region 3 and the two-phase region 4 are the saturated liquid line $x=0$ and saturated vapor line $x=1$; see Figures 3 and 4. A one-dimensional iteration using the IAPWS-IF97 basic equation $f_3^{97}(v,T)$ and the saturation-pressure equation $p_{\mathrm{sat}}^{97}(T)$ is required to calculate the enthalpy or entropy from a given pressure on the saturated liquid or saturated vapor lines of region 3. The boundary equations $p_{3\mathrm{sat}}(h)$ and $p_{3\mathrm{sat}}(s)$, provided in this release, make it possible to determine without iteration whether the given state point is located in the two-phase region 4 or in the single-phase region 3.

The boundary between regions 1 and 3 can be calculated directly from a given pressure p and from $T = 623.15\ \mathrm{K}$ using the IAPWS-IF97 basic equation $g_1^{97}(p,T)$. The boundary between regions 2 and 3 can be calculated directly from given pressure p and from the B23-equation $T = T_{\mathrm{B23}}^{97}(p)$ of IAPWS-IF97 and using the IAPWS-IF97 basic equation $g_2^{97}(p,T)$.

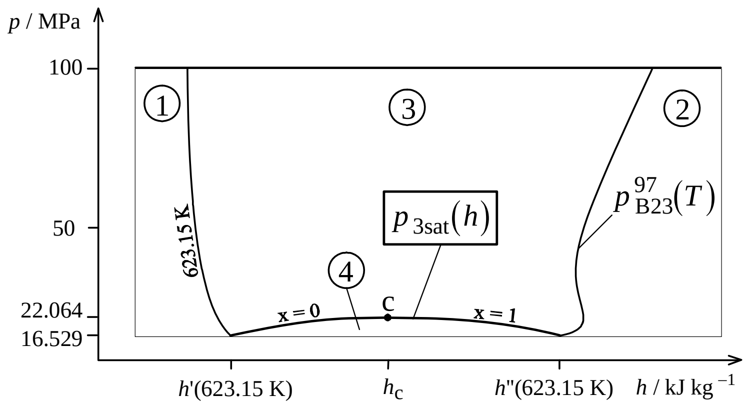

Figure 3. Illustration of IAPWS-IF97 region 3 and the boundary equation $p_{3sat}(h)$ in a *p*-*h* diagram

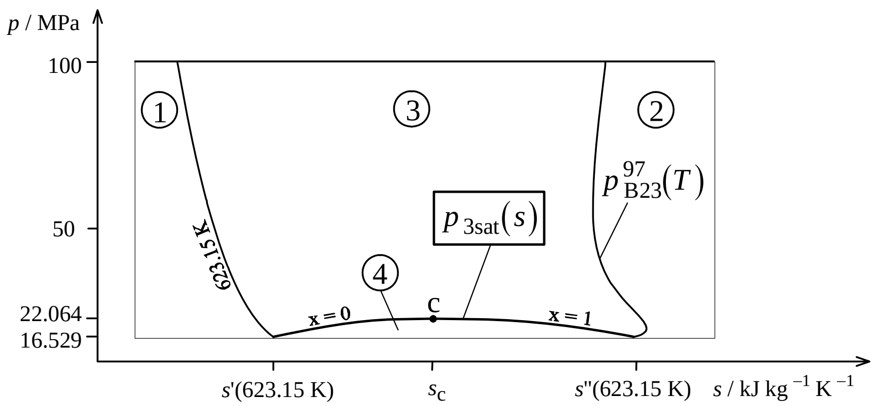

Figure 4. Illustration of IAPWS-IF97 region 3 and the boundary equation $p_{3sat}(s)$ in a *p*-*s* diagram

4.2 Numerical Consistency Requirements

The required consistency of the boundary equations for the saturation lines of region 3 result from IAPWS requirements on backward functions. Therefore, the backward functions $T(p,h)$, $v(p,h)$, $T(p,s)$, and $v(p,s)$ have to fulfill their numerical consistency requirements when using the boundary equations $p_{3sat}(h)$ and $p_{3sat}(s)$ for determining the region of a given state point.

4.3 Boundary Equations $p_{sat}(h)$ and $p_{sat}(s)$

The Equation $p_{3sat}(h)$. The equation $p_{3sat}(h)$ describes the saturated liquid line and the saturated vapor line including the critical point in the enthalpy range (see Figure 3):

$$h'(623.15\ \mathrm{K}) \le h \le h''(623.15\ \mathrm{K}),$$

$$\text{where } h'(623.15\ \mathrm{K}) = 1.670\ 858\ 218 \times 10^3\ \mathrm{kJ\ kg^{-1}},$$
$$\text{and } h''(623.15\ \mathrm{K}) = 2.563\ 592\ 004 \times 10^3\ \mathrm{kJ\ kg^{-1}}.$$

The boundary equation $p_{3\text{sat}}(h)$ has the following dimensionless form:

$$\frac{p_{3\text{sat}}(h)}{p^*} = \pi(\eta) = \sum_{i=1}^{14} n_i\,(\eta - 1.02)^{I_i}\,(\eta - 0.608)^{J_i} \quad , \tag{10}$$

where $\pi = p/p^*$ and $\eta = h/h^*$, with $p^* = 22\ \text{MPa}$ and $h^* = 2600\ \text{kJ kg}^{-1}$. The coefficients n_i and exponents I_i and J_i of Eq. (10) are listed in Table 17.

Table 17. Coefficients and exponents of the boundary equation $p_{3\text{sat}}(h)$ in its dimensionless form, Eq. (10)

i	I_i	J_i	n_i	i	I_i	J_i	n_i
1	0	0	0.600 073 641 753 024	8	8	24	$0.252\ 304\ 969\ 384\ 128 \times 10^{18}$
2	1	1	$-0.936\ 203\ 654\ 849\ 857 \times 10^{1}$	9	14	16	$-0.389\ 718\ 771\ 997\ 719 \times 10^{19}$
3	1	3	$0.246\ 590\ 798\ 594\ 147 \times 10^{2}$	10	20	16	$-0.333\ 775\ 713\ 645\ 296 \times 10^{23}$
4	1	4	$-0.107\ 014\ 222\ 858\ 224 \times 10^{3}$	11	22	3	$0.356\ 499\ 469\ 636\ 328 \times 10^{11}$
5	1	36	$-0.915\ 821\ 315\ 805\ 768 \times 10^{14}$	12	24	18	$-0.148\ 547\ 544\ 720\ 641 \times 10^{27}$
6	5	3	$-0.862\ 332\ 011\ 700\ 662 \times 10^{4}$	13	28	8	$0.330\ 611\ 514\ 838\ 798 \times 10^{19}$
7	7	0	$-0.235\ 837\ 344\ 740\ 032 \times 10^{2}$	14	36	24	$0.813\ 641\ 294\ 467\ 829 \times 10^{38}$

Computer-program verification. To assist the user in computer-program verification of Eq. (10), Table 18 contains test values for calculated pressures.

Table 18. Selected pressure values calculated from Eq. (10)[a]

Equation	h / kJ kg^{-1}	p / MPa
$p_{3\text{sat}}(h)$, Eq. (10)	1700	$1.724\ 175\ 718 \times 10^{1}$
	2000	$2.193\ 442\ 957 \times 10^{1}$
	2400	$2.018\ 090\ 839 \times 10^{1}$

[a] It is recommended that programmed functions be verified using 8 byte real values for all variables.

Equation $p_{3sat}(s)$. The equation $p_{3\text{sat}}(s)$ describes the saturated liquid line and the saturated vapor line including the critical point in the entropy range (see Figure 4):

$$s'(623.15\ \text{K}) \le s \le s''(623.15\ \text{K}),$$

where $s'(623.15\ \text{K}) = 3.778\ 281\ 340\ \text{kJ kg}^{-1}\ \text{K}^{-1}$,
and $s''(623.15\ \text{K}) = 5.210\ 887\ 825\ \text{kJ kg}^{-1}\ \text{K}^{-1}$.

The boundary equation $p_{3\text{sat}}(s)$ has the following dimensionless form:

$$\frac{p_{3\text{sat}}(s)}{p^*} = \pi(\sigma) = \sum_{i=1}^{10} n_i\,(\sigma - 1.03)^{I_i}\,(\sigma - 0.699)^{J_i} \quad , \tag{11}$$

where $\pi = p/p^*$ and $\sigma = s/s^*$, with $p^* = 22\ \text{MPa}$ and $s^* = 5.2\ \text{kJ kg}^{-1}\ \text{K}^{-1}$. The coefficients n_i and exponents I_i and J_i of Eq. (11) are listed in Table 19.

Table 19. Coefficients and exponents of the boundary equation $p_{3\text{sat}}(s)$ in its dimensionless form, Eq. (11)

i	I_i	J_i	n_i	i	I_i	J_i	n_i
1	0	0	0.639 767 553 612 785	6	12	14	$-0.378\ 829\ 107\ 169\ 011 \times 10^{18}$
2	1	1	$-0.129\ 727\ 445\ 396\ 014 \times 10^{2}$	7	16	36	$-0.955\ 586\ 736\ 431\ 328 \times 10^{35}$
3	1	32	$-0.224\ 595\ 125\ 848\ 403 \times 10^{16}$	8	24	10	$0.187\ 269\ 814\ 676\ 188 \times 10^{24}$
4	4	7	$0.177\ 466\ 741\ 801\ 846 \times 10^{7}$	9	28	0	$0.119\ 254\ 746\ 466\ 473 \times 10^{12}$
5	12	4	$0.717\ 079\ 349\ 571\ 538 \times 10^{10}$	10	32	18	$0.110\ 649\ 277\ 244\ 882 \times 10^{37}$

Computer-program verification. To assist the user in computer-program verification of Eq. (11), Table 20 contains test values for calculated pressures.

Table 20. Selected pressure values calculated from Eq. (11)[a]

Equation	s / kJ kg^{-1} K^{-1}	p / MPa
	3.8	$1.687\ 755\ 057 \times 10^{1}$
$p_{3\text{sat}}(s)$, Eq. (11)	4.2	$2.164\ 451\ 789 \times 10^{1}$
	5.2	$1.668\ 968\ 482 \times 10^{1}$

[a] It is recommended that programmed functions be verified using 8 byte real values for all variables.

Numerical Consistency with the Saturation-Pressure Equation of IAPWS-IF97. The maximum percentage deviation between the pressure calculated from the boundary equation $p_{3\text{sat}}(h)$, Eq. (10), and the IAPWS-IF97 saturation-pressure equation $p_{\text{sat}}^{97}(T)$ has the following value

$$\left|\frac{\Delta p}{p}\right|_{\max} = \left|\frac{p_{3\text{sat}}(h) - p_{\text{sat}}^{97}(T)}{p_{\text{sat}}^{97}(T)}\right|_{\max} = 0.00043\ \% \,.$$

The maximum percentage deviation between the calculated pressure $p_{3\mathrm{sat}}(s)$, Eq. (11), and the IAPWS-IF97 saturation-pressure equation $p_{\mathrm{sat}}^{97}(T)$ has the following value

$$\left|\frac{\Delta p}{p}\right|_{\max} = \left|\frac{p_{3\mathrm{sat}}(s) - p_{\mathrm{sat}}^{97}(T)}{p_{\mathrm{sat}}^{97}(T)}\right|_{\max} = 0.0033\,\% .$$

Consistency of the Backward Equations T(p,h), v(p,h), T(p,s), and v(p,s) with the Basic Equation of IAPWS-IF97 along the Boundary Equations $p_{sat}(h)$ and $p_{sat}(s)$. The maximum temperature differences between the backward equations $T_{3\mathrm{a}}(p,h)$, Eq. (2), and $T_{3\mathrm{b}}(p,h)$, Eq. (3), and the IAPWS-IF97 basic equation $f_3^{97}(v,T)$ along the boundary equation $p_{3\mathrm{sat}}(h)$, Eq. (10), in comparison with the permissible differences are listed in Table 21. The temperature differences were calculated as $\Delta T = T_3\left[p_{3\mathrm{sat}}\left(h_3^{97}\right), h_3^{97}\right] - T$. The function T_3 represents the calculation of $T(p,h)$ using the backward equations of subregions 3a and 3b, Eqs. (2) and (3).

Table 21. Maximum differences of temperature and specific volume calculated from Eqs. (2), (3), (4), and (5) from the IAPWS-IF97 basic equation $f_3^{97}(v,T)$ along the boundary equation $p_{3\mathrm{sat}}(h)$, Eq. (10), and related permissible values

Subregion	Equation	$\lvert\Delta T\rvert_{\mathrm{tol}}$	$\lvert\Delta T\rvert_{\max}$
3a	(2)	25 mK	0.47 mK
3b	(3)	25 mK	0.46 mK
Subregion	**Equation**	$\lvert\Delta v / v\rvert_{\mathrm{tol}}$	$\lvert\Delta v / v\rvert_{\max}$
3a	(4)	0.01 %	0.00077 %
3b	(5)	0.01 %	0.0012 %

Furthermore, Table 21 contains the maximum percentage differences of specific volume between the backward equations $v_{3\mathrm{a}}(p,h)$, Eq. (4), and $v_{3\mathrm{b}}(p,h)$, Eq. (5), and the IAPWS-IF97 basic equation $f_3^{97}(v,T)$ along the boundary equation $p_{3\mathrm{sat}}(h)$, Eq. (10). The relative differences of specific volume were calculated as $\Delta v / v = \left(v_3\left[p_{3\mathrm{sat}}\left(h_3^{97}\right), h_3^{97}\right] - v\right) \Big/ v$. The function v_3 represents the calculation of $v(p,h)$ using the backward equations of subregions 3a and 3b, Eqs. (4) and (5).

The maximum temperature differences and the maximum relative differences of specific volume are smaller than the permissible values. Therefore, the numerical consistency of the boundary equation $p_{3\mathrm{sat}}(h)$, Eq. (10), is sufficient.

The maximum temperature differences between the backward equations $T_{3a}(p,s)$, Eq. (6), and $T_{3b}(p,s)$, Eq. (7), and the IAPWS-IF97 basic equation $f_3^{97}(v,T)$ along the boundary equation $p_{3sat}(s)$, Eq. (11), in comparison with the permissible differences are listed in Table 22. The temperature differences were calculated as $\Delta T = T_3\left[p_{3sat}\left(s_3^{97}\right), s_3^{97}\right] - T$. The function T_3 represents the calculation of $T(p,s)$ using the backward equations of subregions 3a and 3b, Eqs. (6) and (7).

Table 22. Maximum differences of temperature and specific volume calculated from Eqs. (6), (7), (8), and (9) to the IAPWS-IF97 basic equation $f_3^{97}(v,T)$ along the boundary equation $p_{3sat}(s)$, Eq. (11), and related permissible values

Subregion	Equation	$\lvert\Delta T\rvert_{tol}$	$\lvert\Delta T\rvert_{max}$
3a	(6)	25 mK	2.69 mK
3b	(7)	25 mK	2.12 mK
Subregion	Equation	$\lvert\Delta v/v\rvert_{tol}$	$\lvert\Delta v/v\rvert_{max}$
3a	(8)	0.01 %	0.0034 %
3b	(9)	0.01 %	0.0020 %

Furthermore, Table 22 contains the maximum percentage differences of specific volume between the backward equations $v_{3a}(p,s)$, Eq. (8), and $v_{3b}(p,s)$, Eq. (9), and the IAPWS-IF97 basic equation $f_3^{97}(v,T)$ along the boundary equation $p_{3sat}(s)$, Eq. (11). The relative differences of specific volume were calculated as $\Delta v/v = \left(v_3\left[p_{3sat}\left(s_3^{97}\right), s_3^{97}\right] - v\right)\big/ v$. The function v_3 represents the calculation of $v(p,s)$ using the backward equations of subregions 3a and 3b, Eqs. (8) and (9).

The maximum temperature differences and the maximum relative differences of specific volume are smaller than the permissible values. Therefore, the numerical consistency of the boundary equation $p_{3sat}(s)$, Eq. (11), is sufficient.

4.4 Computing Time in Relation to IAPWS-IF97

A very important motivation for the development of the equations for saturation lines of region 3 was reducing the computing time to determine the region for a given state point (p,h) and (p,s). In IAPWS-IF97, time-consuming iterations, *e.g.*, the Newton method, are required. By using equations $p_{3sat}(h)$, Eq. (10), and $p_{3sat}(s)$, Eq. (11), the calculation to determine the region is about 60 times faster than that of the two-dimensional Newton method.

5 References

[1] IAPWS, *Revised Release on the IAPWS Industrial Formulation 1997 for the Thermodynamic Properties of Water and Steam* (2007), available from: http://www.iapws.org.

[2] Wagner, W., Cooper, J. R., Dittmann, A., Kijima, J., Kretzschmar, H.-J., Kruse, A., Mareš, R., Oguchi, K., Sato, H., Stöcker, I., Šifner, O., Tanishita, I., Trübenbach, J., and Willkommen, Th., The IAPWS Industrial Formulation 1997 for the Thermodynamic Properties of Water and Steam, *ASME J. Eng. Gas Turbines Power* **122**, 150-182 (2000).

[3] Kretzschmar, H.-J., Cooper, J. R., Dittmann, A., Friend, D. G., Gallagher, J. S., Harvey, A. H., Knobloch, K., Mareš, R., Miyagawa, K., Okita, N., Stöcker, I., Wagner, W., and Weber, I., Supplementary Backward Equations $T(p,h)$, $v(p,h)$, and $T(p,s)$, $v(p,s)$ for the Critical and Supercritical Regions (Region 3) of the Industrial Formulation IAPWS-IF97 for Water and Steam, *ASME J. Eng. Gas Turbines Power* **129**, 294-303 (2007).

[4] IAPWS, *Revised Supplementary Release on Backward Equations for Pressure as a Function of Enthalpy and Entropy p(h,s) for Regions 1 and 2 of the IAPWS Industrial Formulation 1997 for the Thermodynamic Properties of Water and Steam* (2014), available from: http://www.iapws.org.

[5] Kretzschmar, H.-J., Cooper, J. R., Dittmann, A., Friend, D. G., Gallagher, J. S., Knobloch, K., Mareš, R., Miyagawa, K., Stöcker, I., Trübenbach, J., Wagner, W., Willkommen, Th., Supplementary Backward Equations for Pressure as a Function of Enthalpy and Entropy $p(h,s)$ to the Industrial Formulation IAPWS-IF97 for Water and Steam, *ASME J. Eng. Gas Turbines Power* **128**, 702-713 (2006).

[6] Kretzschmar, H.-J., Specifications for the Supplementary Backward Equations $T(p,h)$ and $T(p,s)$ in Region 3 of IAPWS-IF97, in: *Minutes of the Meetings of the Executive Committee of the International Association for the Properties of Water and Steam, Gaithersburg 2001*, ed. by B. Dooley, IAPWS Secretariat (2001), p. 6 and Attachment 7- Item #6.

[7] Rukes, B., Specifications for Numerical Consistency, in: *Minutes of the Meetings of the Executive Committee of the International Association for the Properties of Water and Steam, Orlando 1994*, ed. by B. Dooley, IAPWS Secretariat (1994), pp. 31-33.

[8] Kretzschmar, H.-J., Stöcker, I., Klinger, J., and Dittmann, A., Calculation of Thermodynamic Derivatives for Water and Steam Using the New Industrial Formulation IAPWS-IF97, in: *Steam, Water and Hydrothermal Systems: Physics and Chemistry Meeting the Needs of Industry*, Proceedings of the 13th International Conference on the Properties of Water and Steam, ed. by P. R. Tremaine, P. G. Hill, D. E. Irish, and P. V. Balakrishnan, NRC Press, Ottawa, 2000, pp. 238-247.

[9] Rukes, B., and Wagner, W., Final Set of Specifications for the New Industrial Formulation, in: *Minutes of the Meetings of the Executive Committee of the International Association for the Properties of Water and Steam, Tokyo 1991*, ed. by B. Dooley, IAPWS Secretariat (1991), pp. 78-82.

[10] IAPWS, *Release on the Values of Temperature, Pressure and Density of Ordinary and Heavy Water Substances at their Respective Critical Points* (1992), available from: http://www.iapws.org.